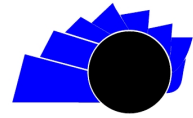




UNIVERSIDAD DISTRITAL
FRANCISCO JOSÉ DE CALDAS



Optimization of part orientation focused on minimizing support structures

Optimización de orientación de pieza enfocado en la minimización de estructuras de soporte

Juan C. Guacheta-Alba ¹, Robinson Jiménez-Moreno ², Anny Espitia Cubillos ³

INFORMACIÓN DEL ARTÍCULO

Historia del artículo:

Enviado: 19/01/2023

Recibido: 21/02/2023

Aceptado: 26/03/2023

Keywords:

3D printing

Tensegrity

Optimization

Assistive robotics

Gripper

Flexible printing



Palabras clave:

Impresión 3D

Tensegridad

Optimización

Robótica asistencial

Impresión flexible

ABSTRACT

The optimization of manufacturing processes has acquired significant importance due to its ability to improve operations and reduce costs and material consumption. In the manufacturing process of specific structures, such as tensegrity structures, there is a high geometric complexity and the presence of internal areas without deposited material, reducing material consumption and the structure's weight. Optimization methods are used to improve the manufacture of structures used in robotic assistance arms to define the piece's orientation and the location of the supports in a 3D printing system. The objective function of this approach is to minimize the volume needed to build the regions that require support, complying with printing restrictions, and ensuring self-support and integrity of the structure. For this, an evolutionary optimization algorithm is used to determine the optimal orientation of the parts, which leads to a direct reduction in the consumption of support material and the final weight of the structure. Also, it presents an improvement in the printing quality of the piece.

RESUMEN

La optimización de los procesos de fabricación y manufactura ha adquirido una importancia significativa debido a su capacidad para mejorar procesos y reducir los costos y el consumo de material. En el proceso de fabricación de ciertas estructuras, como las estructuras de tensegridad representa una alta complejidad geométrica y una presencia de áreas internas sin material depositado, repercutiendo en una reducción en el consumo de material y el peso de la estructura. Con el objetivo de mejorar la fabricación de estructuras utilizadas en brazos robóticos asistenciales, se recurre a métodos de optimización que permiten definir la orientación de la pieza y la ubicación de los soportes en un sistema de impresión 3D. La función objetivo de este proceso es minimizar el volumen necesario para construir las regiones que requieren soporte, cumpliendo con las

- 1 B.Sc. Mechatronics Engineering, Universidad Militar Nueva Granada, Colombia. M.Sc. Mechatronics Engineering, Universidad Militar Nueva Granada, Colombia. PhD student in mechanical engineering: Universidade Federal do Rio de Janeiro, Brazil. E-mail: juan.camilo@mecanica.coppe.ufrj.br
- 2 B.Sc. Electronic Engineering, Universidad Distrital Francisco José de Caldas, Colombia. Ph.D. Engineering, Universidad Distrital Francisco José de Caldas, Colombia. Associate Professor: Universidad Militar Nueva Granada, Colombia. E-mail: robinson.jimenez@unimilitar.edu.co
- 3 Industrial engineering, Universidad Militar Nueva Granada, Colombia. Master's degree in engineering, Universidad de Los Andes, Colombia. Full time teacher: Universidad Militar Nueva Granada, Colombia. E-mail: anny.espitia@unimilitar.edu.co

Citar este artículo como: J. C. Guacheta-Alba, R. Jiménez-Moreno, A. Espitia Cubillos, "Optimization of part orientation focused on minimizing support structures", *Visión electrónica*, vol. 17, no. 2, pp. 220-229, july-december 2023, <https://doi.org/10.14483/22484728.22016>

restricciones de impresión y garantizando el autosoporte y la integridad de la estructura. Para lograr esto, se utiliza un algoritmo de optimización evolutiva para determinar la orientación óptima de las piezas, lo que conlleva a una reducción directa en el consumo de material de soporte, en el peso final de la estructura, y presentando una mejora en la calidad de impresión de la pieza.

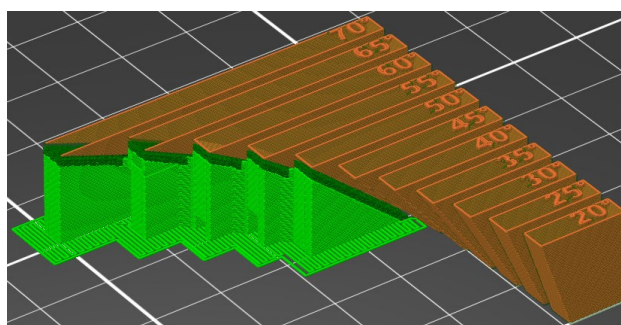
1. Introduction

3D printing systems represent a source of opportunities in both academia and industry. Its applications span a wide range of fields, from creating cutting-edge optical devices [1] to revolutionary advances in architecture [2]. In addition, they extend to the conception and development of highly specialized electronic sensors [3] and the integration of these sensors into state-of-the-art robotic devices [4-5]. They have even become an essential tool for designing and constructing advanced robotic systems [6]. This versatility and capacity for continuous innovation make 3D printing a cutting-edge technology with high potential in various disciplines.

The constant development of 3D printing systems is reflected in a wide range of research and application areas. An outstanding example is the characterization of printing materials, especially relevant in fields such as the manufacture of medical equipment, where quality and safety are fundamental [7]. In addition, optimizing extruder force control in metal printers has been a critical approach to improving the accuracy and quality of printed parts [8]. Also, in plastic inkjet 3D printers, cooling channel optimization has been a critical study area to ensure an efficient and controlled printing process [9]. Finally, planning print paths for structures with low fill weight has become an essential field of research, enabling the creation of lightweight and resistant objects with efficient use of material [10]. These examples illustrate the dynamic and continuous development in which 3D printing systems are immersed, driven by the constant search for improvements and technological advances.

Optimization is a crucial field of research that encompasses a wide range of aspects throughout the 3D printing process. It also includes optimizing the printing material used [11], accelerating the mass production of prototypes [12], developing new properties for printing materials [13-14], as well as improving structural efficiency in the designs to be printed [15]. These are all essential aspects for the continuous improvement of 3D printing systems. In this work, we explore the optimization of the orientation of the printing of parts used to print non-uniform structures or those that, due to their inclination, do not have direct contact with the printing surface, making use of the property of self-support of material that can be observed in Figure 1. The main objective is to reduce the material used in this process and analyze its impact on printing time.

Figure 1. Support material at overhang test part.



Source: [thingiverse.com/thing:40382](https://www.thingiverse.com/thing:40382)

In this paper, the optimization of the orientation of the parts for 3D printing is addressed since this parameter is a criterion defined by the user. A multivariate optimization technique is used to find the optimal orientation. Section 2 describes the methodology employed to reduce the use of support material through correct orientation in part printing

using multivariable optimization algorithms. Section 3 presents a gallery of pieces that comprise the case study to be analyzed. In section 4, the results obtained by applying the orientation optimization methodology to this set of parts are presented, analyzed, and validated using commercial software. Finally, section 5 summarizes the conclusions obtained.

2. Method

This section presents the proposed methodology to directly calculate the amount of support material needed in the 3D printing process. This calculation is based on the 45-degree self-support angle rule for material deposition manufacturing. The application of this calculation is versatile and can be performed on any object, depending on its orientation. The optimization method is described below, which will be applied to calculate the optimal support volume. This volume is defined as the multivariable objective function.

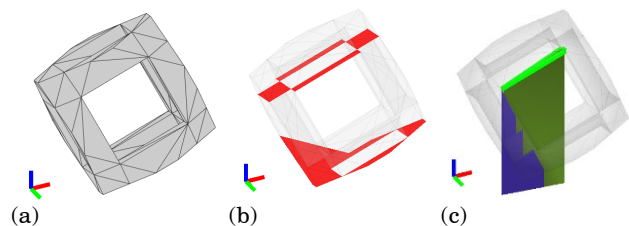
2.1 Problem definition

Initially, the triangles at the bottom are identified according to the selected orientation of the piece. These triangles are critical as they represent surface sections requiring support during printing. For this, the normal vector of each face of the model is calculated based on its triangular representation. This normal vector is obtained by the cross-product operation between two vectors corresponding to the sides of each triangle being analyzed. This vector is a criterion for determining whether a specific region needs support during printing. The angle between the normal vector and the z-axis is measured using the point product operation between these two vectors, as described in Equation 1. In this equation, v_1 and v_2 represent the unit vectors corresponding to sides 1 and 2 of the triangle, respectively, while v_z symbolizes the unit vector of the z-axis.

$$\theta = \cos^{-1}((v_1 \cdot v_2) \times v_z) \quad (1)$$

Considering the angle of inclination inherent in the self-support process in 3D printing, a selection of faces that present a calculated angle concerning the z-axis less than 45 degrees is carried out since these are the ones that require reinforcement by adding additional material. Once these faces that need support have been identified, the volume needed to support this specific area is calculated. This calculation process is divided into two stages: In the first stage, the total volume of the region below the analyzed triangle is calculated. In the second stage, the volume of the triangular regions at the bottom of the analyzed triangle is determined, which can act as a support for printing. The final estimate of the material required to maintain this triangle is obtained by subtracting the volume calculated in the first stage from the volume determined in the second stage. Figure 2 shows a final prism on which the calculation will be performed for one of the faces of a part. The representation in green corresponds to the first stage and in blue to the second. Importantly, these stages are repeated cyclically for each area that requires support.

Figure 2. Visualization of the required support volume estimation (a) Part analyzed, (b) Selection of faces to be supported, (c) Support volume calculation.



Source: Own.

In the first stage, we calculate the volume of a prism generated by projecting the triangle of the face on the xy plane. Initially, Equation 2 is used, in which A_{xy} represents the area of the evaluated triangle projected onto the xy plane. This area is obtained by the point product operation between two triangle vectors, excluding their components on the z-axis.

Furthermore, in this equation, \bar{h} denotes the average value of the components on the z-axis of the triangle's vertices. This value represents the uninclined prism that has the same volume. It is worth mentioning that this calculation can be applied to any triangle in space, and its definition will be used later in the calculation of the volume of the second stage.

$$V_A^i = A_{xy}^i \cdot \bar{h}^i \quad (2)$$

Finally, these two volumes will be calculated for all the faces identified as needing support. The support volume for each region will be determined as the difference between the volume of the first and second stages, as indicated in Equation 5. This sum represents the total volume that needs to be covered with support material and is therefore defined in this paper as the objective function of the optimization process.

$$V_B^i = \sum_{i=1}^{num\ of\ faces} A_{xy}^{intersect\ i} \cdot \bar{h}^{*i} \quad (3)$$

Finally, these two volumes will be calculated for all the faces identified as needing support. The support volume for each region will be determined as the difference between the volume of the first and second stages, as indicated in Equation 5. This sum represents the total volume that needs to be covered with support material and is therefore defined in this paper as the objective function of the optimization process

$$V_{support} = \sum_{i=1}^{num\ of\ faces} V_A^i - V_B^i \quad (4)$$

2.2 Optimization strategy

Initially, the triangles at the bottom are identified according to the selected orientation of the piece. These triangles are critical as they represent surface sections requiring support during printing. For this, the normal vector of each face of the model is calculated based on its triangular representation. This normal vector is obtained by the cross-product operation between two vectors corresponding to the sides of each triangle being analyzed. This vector is a criterion for

determining whether a specific region needs support during printing. The angle between the normal vector and the z-axis is measured using the point product operation between these two vectors, as described in Equation 1. In this equation, v_1 and v_2 represent the unit vectors corresponding to sides 1 and 2 of the triangle, respectively, while v_z symbolizes the unit vector of the z-axis.

To reduce the material deposited in the 3D printing process, it is proposed to minimize the support volume of the parts, which is directly related to the deposited support material. To structure the problem, the three angles of rotation, roll (φ), pitch (θ) and yaw (ψ), also called navigation angles or Tait-Bryan angles, are defined as decision variables. To describe the orientation of the part in space, a rotation matrix called the R_{RPY} matrix is used, which is defined in (5). In this matrix, R_z , R_y , and R_x are the rotations around the z, y, and x axes, respectively. This matrix is applied to each vertice that constitutes the piece, and through different combinations of these rotations, all possible orientations of the solid object can be achieved.

$$R_{RPY} = R_{z,\varphi} R_{y,\theta} R_{x,\psi} \quad (5)$$

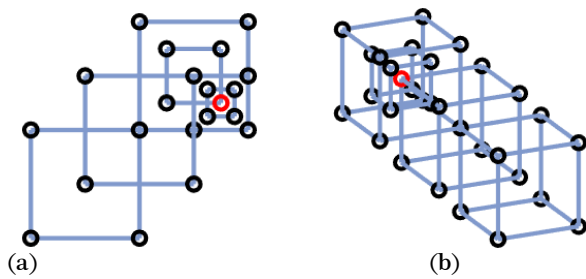
Mathematically, the part orientation optimization process is defined by Equation 6. In this equation, x represents the vector formed by the Tait-Bryan angles of the rotation matrix R_{RPY} , while the objective function is previously expressed in Equation 5. It should be noted that the search space, denoted as S , is defined for each decision variable in an interval ranging from 0 to 2π .

$$\min f(x) \text{ where } x = \{\varphi, \theta, \psi\} \in S \subseteq \mathbb{R}^3 \quad (6)$$

As presented in the first section, several multivariate optimization algorithms can be applied to the problem. Given the applications and results obtained, the evolutionary operation algorithm is selected to evaluate the current case. The evolutionary

operation method, also known as EVOP, was proposed by George Box as a statistical method for process improvement [16]. Their focus lies in adjusting the process or experiment in a direction that leads to improvements within a given workspace. This technique is suitable to be applied in simple problems with two or three decision variables and when seeking to minimize computational requirements regarding calculations and costs.

Figure 3. Process of search of evolutionary operation method for (a) two decision variables (b) three decision variables.



Source: own.

Algorithm 1. Evolutionary operation pseudocode.

Procedure Evolutionary operation

Input: $f(x)$; x_0 ; Δ ; ϵ ; N .
Output: x_{min}

1. $\bar{x} \leftarrow x_0$
2. **if** $||\Delta|| < \epsilon$ **then**
3. $x_{min} \leftarrow \bar{x}$
4. **exit**
5. **else**
6. create 2^N points by adding and subtracting $\Delta_i/2$ from each variable at point \bar{x}
7. calculate $f(x)$ in the (2^N+1) points
8. $\bar{x} \leftarrow$ point with the lowest function value
9. **if** $\bar{x} = x_0$ **then**
10. $\Delta_i \leftarrow \Delta_i / 2$
11. **goto** 2
12. **else**
13. $x_0 \leftarrow \bar{x}$
14. **goto** 2

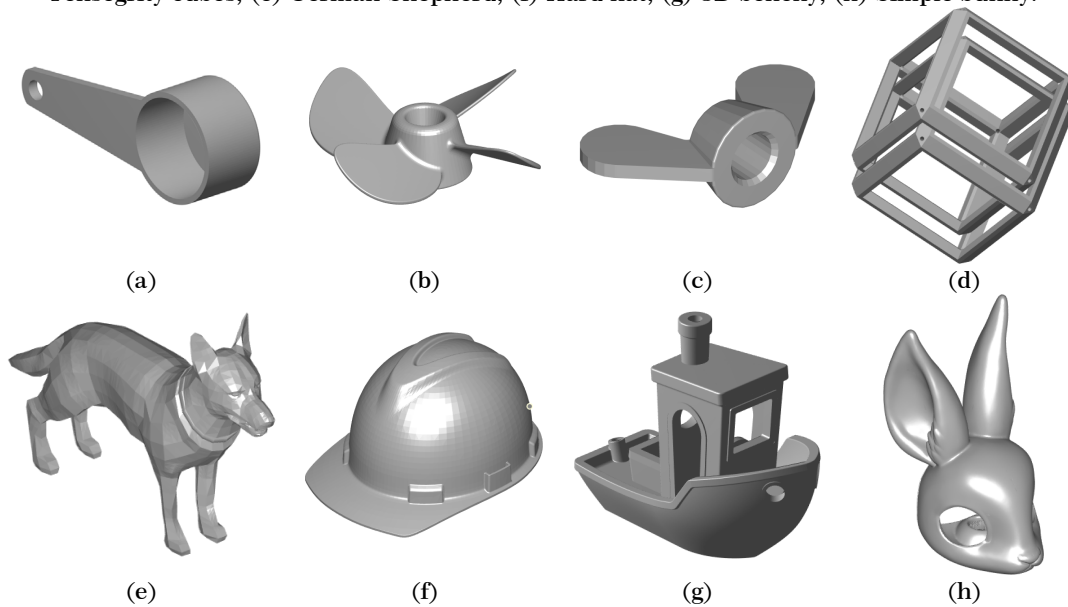
This method uses a set of points equal to (2^N+1) , where N represents the number of decision variables. Of these points, 2^N corresponds to the corners of a hypercube. The function values at the (2^N+1) points are evaluated, and the best point is identified. If, during any iteration, the current point cannot be improved, the size of the hypercube is reduced. To carry out this task, Algorithm 1 shows the pseudocode used for the programming of the evolutionary operation algorithm. In the case of this particular study, the parameters set are a tolerance (ϵ) of 1×10^{-4} and a size reduction vector (Δ) defined as $[1,1,1]$ for the decision variables $[\varphi, \theta, \psi]$.

3. Case study

Figure 4 presents a collection of eight parts to which the part orientation optimization algorithm will be applied. The purpose is to evaluate the target function and the chosen optimization strategy. These pieces were selected from those available under Creative Commons license and feature a variety of surfaces and textures. The objective is to evaluate how the orientation calculation behaves and its corresponding optimization in these cases.

Measurements and calculations are made using the dimensions provided by the designer for the parts, which may result in variations in the calculated volumes. Therefore, both volumes are presented in the initial and optimal configuration for an accurate comparison. The programming and execution of the algorithms were carried out using MATLAB 2022 software with a student license on a computer equipped with Intel® Core™ i7-4790 CPU @ 3.60GHz and 24GB RAM.

Figure 4. Piece designs used for optimization (a) Measuring cup, (b) 4 bladed Propeller, (c) Din M8, (d) Tensegrity cubes, (e) German Shepherd, (f) Hard hat, (g) 3D benchy, (h) Simple bunny.



Source: Own.

4. Results and discussion

This section will present the results of executing the part orientation optimization algorithm for the abovementioned models. Table 1 shows the optimal part orientation values, the initial estimated support volume, and the optimal final volume. The optimal orientation values correspond to the Tait-Bryan angles defined in the objective function. Similar optimal orientations were found for the pieces "Measuring cup", "3D benchy" and "Simple bunny", which were studied by past optimization techniques [17]. In terms of calculated support volume, an average reduction of

62% was achieved for the parts evaluated. This results in lower material consumption during the printing process. However, it is essential to note that, due to the geometric complexity, relatively high consumption of support material in several possible orientations is still necessary, like for the "4 bladed Propeller" part. However, it can be guaranteed at least a reduction of 31%.

Subsequently, in Figure 5, the eight pieces are presented in their optimal orientations, and a visualization of the support material required for each of them is represented in green. It is important to note

Table 1. Orientations and volumes obtained for the parts.

Pieces	ϕ [rad]	θ [rad]	ψ [rad]	Initial volume [mm ³]	Final volume [mm ³]
Measuring cup	4.9812	0.7854	0.2946	2.300×10^4	5.128×10^3
4 bladed Propeller	1.7120	0.6227	2.3626	1.620×10^2	1.113×10^2
Din M8	5.2054	5.5948	5.1227	2.062×10^3	1.512×10^2
Tensegrity cubes	1.1830	5.0706	0.9526	1.851×10^4	7.697×10^3
German Shepherd	3.9203	6.2729	0.6686	9.314×10^6	4.614×10^6
Hard hat	0.9156	2.9618	1.4619	1.873×10^6	2.664×10^5
3D benchy	5.9326	0.7561	0.6157	8.307×10^3	5.178×10^3
Simple bunny	5.8785	0.0246	5.6941	8.218×10^3	2.907×10^3

Source: own.

that for selected geometries, these orientations differ from those predetermined by the designers and are mostly not aligned parallel to one of the faces of the model. In these results, particularly evident in the solids "Measuring cup", "Din M8" and "3D benchy", there is a predominant tendency to tilt the model at an angle of 45 degrees with respect to the xy plane. This is due to the rule taken into account in the programming that allows this inclination, which allows self-support in some areas of the models.

In order to evaluate both the performance of the programmed function and the optimization algorithm, the execution times and the number of iterations required to obtain the optimal orientation in each execution have been measured. These metrics are detailed in Table 2, together with the number of faces that make up the model. It should be noted that a mesh reorganization was performed in some cases with many faces. As expected, models with fewer faces

tended to have shorter calculation times. However, geometry also influenced the calculation time since this increased in the presence of hollow regions or holes within the model, as observed in the cases of "Tensegrity cubes", "3D benchy" and "Simple bunny". Compared to previous studies, the calculation time has been increased due to the greater complexity and accuracy of the target function used to estimate the support volume, verified on the commercial

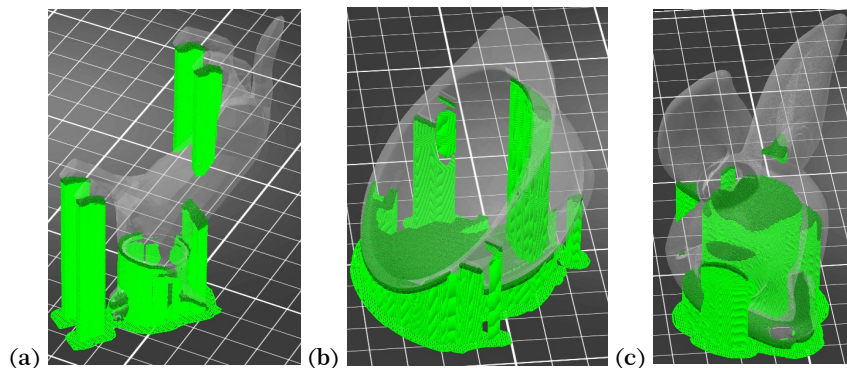
Once the optimal orientations are obtained, they are exported to the PrusaSlicer printing software to validate the minimization of support material in the printing process. In Figure 6 are presented in green the regions in which the deposited support material for three models in their optimal orientations found. As can be observed, these results present similar regions to those presented in Figure 5, corroborating the correct calculation of the support material and evaluating the applicability of self-support in printing.

Table 2. Computational information of algorithm executions.

Pieces	Number of faces	Number of iterations	Execution time [s]
Measuring cup	490	31	39.1384
4 bladed Propeller	512	33	92.4081
Din M8	534	38	41.0938
Tensegrity cubes	676	69	392.2985
German Shepherd	834	39	195.9186
Hard hat	1094	38	226.8086
3D benchy	1576	42	551.5912
Simple bunny	1656	27	269.9786

Source: Own.

Figure 6. Visualization of support material for parts in optimal orientations by PrusaSlicer (a) German Shepherd, (b) Hard hat, (c) Simple bunny.



Source: own.

The PrusaSlicer software also allows for determining the length and mass used as support material and providing information on the time required for its deposition.

Comparing the amount of support material with the values obtained for the initial orientations, which correspond to the orientations provided in Figure 6, an average reduction of 41% is observed in the amount of material used in the mass and length of the parts analyzed. It should be noted that this reduction was lower in the case of the piece "Tensegrity cubes" (7%) and significantly higher in the piece "Din M8" (85%). In addition, the printing time of the support material was reduced on average by 26% in the selected models. This value is lower than those presented above in mass and volume since the printing time depends on the number of layers used in the printing process, and tilting the part can increase the number of layers required. For certain parts, such as "Tensegrity cubes" and "3D benchy", the supporting material's printing time is longer than its initial orientation. However, in

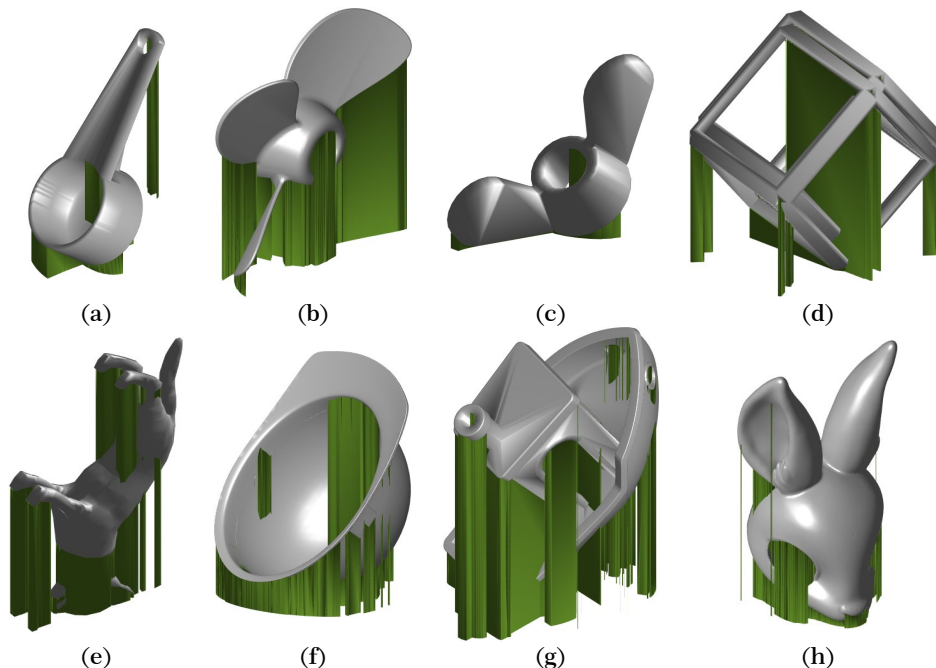
all models, an effective reduction of the material used is achieved.

5. Conclusions

An algorithm has been developed to optimize the part's orientation intended for printing by material deposition. This algorithm allows a previous stage of adjustment in the arrangement of the part, which leads to a significant reduction in the amount of support material needed during manufacturing, which translates into a decrease in production costs. The methodology presented can accurately calculate the volume required to support parts with highly complex geometries in any conceivable orientation. Through the use of an operational evolution algorithm, the optimal configuration for printing is selected.

This methodology considers the self-support capacity that can be achieved in material deposition printing, which is a design parameter and can be

Figure 5. Optimal results for pieces (a) Measuring cup, (b) 4 bladed Propeller, (c) Din M8, (d) Tensegrity cubes, (e) German Shepherd, (f) Hard hat, (g) 3D benchy, (h) Simple bunny.



Source: Own.

chosen by the user. It is important to note that this process can be applied to parts of any geometry. The support volume was minimized between 31% and 92% for the solids presented. This was confirmed using the PrusaSlicer software, where minimizing the support material in a range varying between 8% and 85% was possible. At all times, a significant reduction in material usage is guaranteed.

It is recommended to use optimization strategies in the preprocessing phase of 3D printing to determine the optimal orientation of the parts when it is not possible to do so visually. This brings benefits such as cost reduction and efficient use of the material. A multi-objective optimization, including printing time, can be considered since the support material and printing time metrics are dependent. STL models are employed due to their wide adoption and continued use in additive manufacturing processes. However, for future work, the possibility of implementing new formats such as .obj or .fbx is contemplated, which are gaining popularity in their use. In addition, in the future, the implementation of parallel programming will be considered to accelerate the calculation of the volume estimate.

Acknowledgments

The authors express their gratitude to the Universidad Militar Nueva Granada for the time provided for the elaboration of this work-2023.

References

- [1] H. Gao, J. An, C. K. Chua, D. Bourell, C. N. Kuo, D. T. Tan, "3D printed optics and photonics: Processes, materials and applications," *Materials Today*, 2023. <https://doi.org/10.1016/j.mattod.2023.06.019>
- [2] C. Wu, L. Wu, G. Shang, H. Guo, "Application and Research of 3D Printing Technology in the Field of Architecture," 2021 4th International Conference on Electron Device and Mechanical Engineering (ICEDME)*, Guangzhou, China, 2021, pp. 71-74, <https://doi.org/10.1109/ICEDME52809.2021.00024>
- [3] J. Oprel, G. Wolterink, J. Schilder, G. Krijnen, "Novel 3D printed capacitive shear stress sensor," *Additive Manufacturing*, Volume 73, 2023. <https://doi.org/10.1016/j.addma.2023.103674>
- [4] J. Ren, F. Wu, E. Shang, D. Li, Y. Liu, "3D printed smart elastomeric foam with force sensing and its integration with robotic gripper," *Sensors and Actuators A: Physical*, Volume 349, 2023. <https://doi.org/10.1016/j.sna.2022.113998>
- [5] G. L. Goh, W. Y. Yeong, J. Altherr, J. Tan, D. Campolo, "3D printing of soft sensors for soft gripper applications," *Materials Today: Proceedings*, vol. 70, 2022, pp. 224-229. <https://doi.org/10.1016/j.matpr.2022.09.025>
- [6] W. Zhang, J. Li, H. Liu, G. Jin, "Research on Embedded 3D Printing for Magnetic Soft Robots," 2021 IEEE 16th International Conference on Nano/Micro Engineered and Molecular Systems (NEMS), Xiamen, China, 2021, pp. 518-523, <https://doi.org/10.1109/NEMS51815.2021.9451436>
- [7] M. Abouelmajd, A. Bahlaoui, I. Arroub, M. Lagache, S. Belhouideg, "Mechanical Characterization of PLA Used in Manufacturing of 3D Printed Medical Equipment for COVID-19 Pandemic," 2020 IEEE 2nd International Conference on Electronics, Control, Optimization and Computer Science (ICECOCS), Kenitra, Morocco, 2020, pp. 1-5, <https://doi.org/10.1109/ICECOCS50124.2020.9314444>

- [8] S. Zhang, G. Xia, X. Hao, Y. Zhang, W. Chen, Z. Zhou, "Design Optimization and Simulation Analysis of Screw Extrusion 3D Printing Screw," 2022 5th World Conference on Mechanical Engineering and Intelligent Manufacturing (WCMEIM), Ma'an Shan, China, 2022, pp. 400-404, <https://doi.org/10.1109/WCMEIM56910.2022.10021447>
- [9] B. B. Kanbur, S. Shen, Y. Zhou, F. Duan, "Neural network-integrated multiobjective optimization of the 3D-printed conformal cooling channels," 2020 5th International Conference on Smart and Sustainable Technologies (SpliTech), Split, Croatia, 2020, pp. 1-6, <https://doi.org/10.23919/SpliTech49282.2020.9243730>
- [10] D. Wang, H. Wang, Y. Wang, "Continuity Path Planning for 3D Printed Lightweight Infill Structures," 2021 IEEE Conference on Telecommunications, Optics and Computer Science (TOCS), Shenyang, China, 2021, pp. 959-962, <https://doi.org/10.1109/TOCS53301.2021.9688877>
- [11] M. H. Ali, G. Yerbolat, S. Amangeldi, "Material Optimization Method in 3D Printing," 2018 IEEE International Conference on Advanced Manufacturing (ICAM), Yunlin, Taiwan, 2018, pp. 365-368, <https://doi.org/10.1109/AMCON.2018.8614886>
- [12] R. F. Peng, "Prototyping to Mass Production: Automated CAD Model and G-Code Optimization Framework for Industrial 3D Printing," 2023 9th International Conference on Mechatronics and Robotics Engineering (ICMRE), Shenzhen, China, 2023, pp. 203-206, <https://doi.org/10.1109/ICMRE56789.2023.10106588>
- [13] M. Bhayana, J. Singh, A. Sharma, M. Gupta, "A review on optimized FDM 3D printed Wood/PLA bio composite material characteristics," Materials Today: Proceedings, 2023. <https://doi.org/10.1016/j.matpr.2023.03.029>
- [14] A. Rabinowitz, P. M. DeSantis, C. Basgul, H. Spece, S. M. Kurtz, "Taguchi optimization of 3D printed short carbon fiber polyetherketoneketone (CFR PEKK)," Journal of the Mechanical Behavior of Biomedical Materials, Volume 145, 2023. <https://doi.org/10.1016/j.jmbbm.2023.105981>
- [15] M. Mogra, O. Asaf, A. Sprecher, O. Amir, "Design optimization of 3D printed concrete elements considering buildability," Engineering Structures, Volume 294, 2023, 116735, ISSN 0141-0296, <https://doi.org/10.1016/j.engstruct.2023.116735>
- [16] G. P. Box, "Evolutionary Operation: A Method for Increasing Industrial Productivity," Journal of the Royal Statistical Society. Series C (Applied Statistics), vol. 6, no. 2, 1957, pp. 81-101, <https://doi.org/10.2307/2985505>
- [17] J. C. Guacheta-Alba, S. Gonzalez, D. A. Nunez, M. Mauledoux, O. Aviles, "3D printing part orientation optimization: discrete approximation of support volume," International Journal of Electrical and Computer Engineering, 2022, Vol 12. pp. 5958-5966. <https://doi.org/10.11591/ijece.v12i6.pp5958-5966>